Nutritional Stimulation by *In-ovo* Feeding Modulates Cellular Proliferation and Differentiation in the Small Intestinal Epithelium of Chicks

Naama Reicher
Hebrew University Faculty of Agriculture: Hebrew University of Jerusalem Robert H Smith Faculty of Agriculture Food and Environment

Tal Melkman-Zehavi
Hebrew University Faculty of Agriculture: Hebrew University of Jerusalem Robert H Smith Faculty of Agriculture Food and Environment

Jonathan Dayan
Hebrew University Faculty of Agriculture: Hebrew University of Jerusalem Robert H Smith Faculty of Agriculture Food and Environment

Eric A. Wong
Virginia Tech: Virginia Polytechnic Institute and State University

Zehava Uni (zehava.uni@mail.huji.ac.il)
Hebrew University Faculty of Agriculture: Hebrew University of Jerusalem Robert H Smith Faculty of Agriculture Food and Environment

---

Research

Keywords: chick, intestinal development, proliferation, differentiation, multipotent cells, In-ovo feeding, glutamine, leucine

Posted Date: February 2nd, 2021

DOI: https://doi.org/10.21203/rs.3.rs-178831/v1

Version of Record: A version of this preprint was published at Animal Nutrition on September 1st, 2021.
See the published version at https://doi.org/10.1016/j.aninu.2021.06.010.

Abstract

Background

Nutritional stimulation of the small intestine (SI) of chick embryos can be conducted by enriching the amniotic fluid with nutrients via the in-ovo feeding (IOF) methodology. The impact of IOF of specific nutrients on cellular proliferation and differentiation within the multipotent (MP) and differentiated cell niches of the developing SI have not yet been characterized. In the study, we examined the effects of IOF of 1% glutamine (IOF-Gln), 1% leucine (IOF-Leu) and 0.4% NaCl (IOF-NaCl), compared to non-injected controls, on the proportions and localizations of MP, progenitor and differentiated cells within the SI epithelium of peri-hatch chicks. MP, progenitor and differentiated cells were located and quantified in jejunum sections of all treatment groups at E17 and at E19, and post-hatch at days 0, 1, 3 and 7, by immunofluorescence of Sox9 and PCNA, in-situ hybridization of Lgr5 and PepT1 and histochemical goblet cell staining.

Results

At E19, 48 h post IOF, the effects of IOF treatments, in comparison to Control embryos, were as follows: total cell counts increased by 40%, 33% and 19%, and MP cell counts increased by 52%, 50% and 38%, in IOF-Gln, IOF-Leu and IOF-NaCl embryos, respectively. Only IOF-Gln embryos exhibited a significant, 36% increase in progenitor cell counts. Lgr5+ stem cell localizations shifted to villus bottoms in IOF-treated embryos. The differentiated, PepT1+ region of the villi was 1.9 and 1.3-fold longer in IOF-Gln and IOF-Leu embryos, respectively, while goblet cell densities decreased by 20% in IOF-Gln embryos. Between hatch and D7, crypt and villi epithelial cell counts were significantly higher IOF-Gln chicks, compared to Control chicks ($P<0.05$).

Conclusions

IOF promotes pre-hatch SI maturation through increased proportions and enhanced compartmentalization of the MP and differentiated cell niches. IOF of glutamine stimulates SI maturation to a greater extent than leucine and NaCl, and elicits further expansions of the crypt and villus epithelium during the first week post-hatch. These findings shed light on the link between primary nutritional stimulation and cellular maturation within the SI epithelium.

Background

The mucosal lining of the small intestine (SI) is a highly functional epithelium comprised of absorptive, secretive and sensory cells, which are constantly renewed by multipotent (MP) intestinal stem cells (ISCs). ISCs reside within crypts, and constantly proliferate for self-renewal and generation of progenitor cells, which differentiate into the functional cells that line lumen-facing villi (1, 2).

Compartmentalization of the MP and differentiated regions of the SI epithelium occurs during villi formation, through a polarized mesenchymal BMP signaling gradient which limits all proliferative, Wnt responsive ISCs to the bottom regions of the developing villi. These regions develop into crypts as the SI matures, while villi become exclusively populated by differentiated cells (2–4). In chicken embryos (Gallus gallus), villi formation occurs at the 15th day of embryonic development (E15), and crypts develop at E21 (day of hatch, DOH) (5–7). Post-hatch, initial feeding stimulates the completion of SI maturation through expansions of the crypt and villus epithelium, mediation of cellular proliferation and differentiation and activation of nutrient transporters, digestive enzymes and mucin secretion (5, 6, 8–11).

SI development can also be enhanced prior to hatch by nutritional stimulation, through *in-ovo* feeding (IOF). IOF is a method for supplying nutrients to the SI of chicken embryos by injecting their amniotic fluid with a formulated nutrient solution at E17, prior to amniotic ingestion, which occurs up until DOH (12–14). Various studies showed that IOF of specific nutrients enhanced peri-hatch intestinal development and functionality by expanding villi and crypt dimensions and increasing nutrient digestion and absorption capacities (15–21).

However, no study to date has examined the effects of *in-ovo* administered nutrients on the dynamics of cellular multipotency, proliferation and differentiation in the SI epithelium of peri-hatch chicks. Evaluating the capacity of IOF for modulating the MP and differentiated compartments of the developing SI will provide important tools for understanding the link between primary nutritional stimulation and cellular characteristics of the SI epithelium.

In this study, we examined the effects of *in-ovo* administration of glutamine and leucine on the localizations and proportions of MP, progenitor and differentiated cells in the SI epithelium of peri-hatch chicks. Glutamine and leucine were chosen for this study based on their well-documented stimulatory effects on SI epithelial cell proliferation through mitogen-activated protein kinase (MAPK) and mechanistic Target of Rapamycin (mTOR) signaling pathways (22–24), which result in improved SI morphology in various animal models, including humans (25), pigs (26, 27) and chicken (28, 29).

Visualizing the pre-hatch SI epithelium, we distinguished between proliferative MP cells, which co-expressed Proliferating Cell Nuclear Antigen (PCNA) (30) and SRY-box transcription factor 9 (Sox9), a marker for Wnt-responsive intestinal MP cells (31), and proliferating progenitor cells located above them, which were PCNA-positive, but did not express Sox9. The effects of IOF on the quantities and percentages of these cells were evaluated 48h post nutrient administration, as well as at DOH, D1, D3 and D7. We further examined the effects of IOF on SI epithelial development by determining the extent of compartmentalization of stem and differentiated cells within the peri-hatch SI epithelium by *in-situ* expression of stem cell marker Leucine-Rich Repeat Containing G-Protein Coupled Receptor 5 (Lgr5) (32), absorptive cell marker SLC15A1/Peptide Transporter 1 (PepT1) (33) and goblet cell mucin staining.

Materials And Methods

Incubation, in-ovo feeding and housing

Fertile broiler eggs (Cobb 500, n = 150) were obtained from a commercial hatchery (Brown Ltd., Hod-Hasharon, Israel) at day of lay and incubated in a Petersime hatcher at the Faculty of Agriculture of the Hebrew University, under standard conditions (37.8°C, 60% relative humidity). Egg viability was examined by candling at the 14th day of incubation (E14) and unviable eggs were discarded. At E17, eggs were divided into four treatment groups (n = 32 each) of similar equal weights (64.5 g ± 4.1 SD) for IOF procedures. All eggs were placed at room temperature (RT) during in-ovo feeding (IOF) procedures and disinfected by spraying of 75% ethanol. Intra-amniotic administration of 0.6ml sterile nutrient solutions, using a 21-gauge needle, was conducted as described in previous studies (12, 16, 34), in three groups, while eggs of the Control group were not injected. Nutrient solutions used were 1) 1% (wt/vol) l-glutamine (Sigma Aldrich, Rehovot, Israel) in 0.4% NaCl (IOF-Gln); 2), 1% (wt/vol) l-leucine (Sigma Aldrich, Rehovot, Israel) in 0.4% NaCl (IOF-Leu); 3) 0.75% NaCl as an injected control (IOF-NaCl). Concentrations in the IOF-Gln and IOF-NaCl groups were chosen according to previous studies of *in-ovo* administrations of amino acids (19, 20). NaCl concentrations in all IOF groups were adjusted for optimal osmolarity of 160–180 mOsmol and pH of 5.4–5.9. Therefore, the IOF-NaCl was injected with a higher concentration of NaCl, compared to the IOF-Gln and IOF-Leu groups.

After IOF procedures, eggs were sprayed again with 75% ethanol and placed back into the hatchery, in hatching trays. Hatching window was monitored from E20, and chicks that hatched between E20.5 and E21 were marked according to their treatment group and transferred to brooder facilities at the Faculty of Agriculture of the Hebrew University. Chicks were raised for 7d with free access to water and to commercial starter feed (Brown feedmill, Kaniel, Israel), formulated according to NRC (National Research Council, 1994) recommendations.

Tissue Sampling

For embryonic intestinal sampling, 6 embryos were randomly selected prior to IOF at E17, and 6 embryos were randomly selected from each treatment group at E19 (48 h post IOF procedures). Post-hatch intestinal sampling was conducted on 6 randomly selected chicks from each treatment group at day of Hatch (DOH) and D1, D3 and D7 (treatment groups and sampling timepoints are depicted in Fig. 1). Embryos were euthanized by cervical dislocation and chicks were euthanized by CO2, according to established guidelines for animal care and handling by the Hebrew University Institutional Animal Care and Use Committee (IACUC:AG-17-15355-2). The jejunum segment of their small intestines (a 0.5-1cm piece from the midpoint between the duodenal loop and Meckel's diverticulum) was excised, lumen contents were flushed out with PBS and tissues were fixed in 3.7% formaldehyde in PBS (pH 7.4) for 24h at room temperature (RT). Following fixation, tissues were dehydrated in graded series of ethanol, cleared by Histochoice® (Sigma-Aldrich, Rehovot, Israel) and embedded in Paraplast® (Sigma-Aldrich, Rehovot, Israel). Tissue blocks were sectioned 5µm thick with a microtome, and mounted on SuperFrost Plus™ glass slides (Bar-Naor Ltd., Petah-Tikva, Israel).

Immunofluorescence

Jejunum sections were deparaffinized by Histochoice® (Sigma-Aldrich, Rehovot, Israel) and rehydrated in a graded series of ethanol. Antigen retrieval was then performed by heating for 20 minutes in pH 5.5 citrate buffer (Sigma-Aldrich, Rehovot, Israel). Tissue permeabilization was conducted with 0.1% Tween® (Sigma-Aldrich, Rehovot, Israel) in PBS (PBST). Following incubation in a blocking solution of 1% bovine serum albumin (BSA, Sigma-Aldrich, Rehovot, Israel) in PBS, tissues were incubated overnight at 4□C with rabbit anti-Sox9 (1:150, AB5535, Millipore) and mouse anti-PCNA (1:300, sc-56, Santa Cruz) primary antibodies. Tissues were then washed in PBS and PBST, and then incubated for 1 hour at RT with donkey anti-Rabbit Alexa Fluor 488 (1:100, 711-545-152, Jackson ImmunoResearch Laboratories, Inc.) and donkey anti-mouse Cy3 (1:100, 715-165-150, Jackson ImmunoResearch Laboratories, Inc.) secondary antibodies. Lastly, tissues were washed in PBS and sealed with Fluoromount G with 4',6-diamidino-2-phenylindole (DAPI) (00-4959, Invitrogen).

Cell Sub-Type Quantification

Images were acquired by BX40 Olympus microscope (Waltham, MA, USA) at X400 magnification with a DP73 camera and processed in cellSense Imaging Software (version 1.16). For full-length images of post-hatch villi, images were acquired by EVOS® FL Auto Imaging System (Thermo Fisher Scientific) at X200 magnification and automatically stitched. All images were post-processed for brightness/contrast adjustments and channel merging using ImageJ software. Cellular quantification in embryonic villi was conducted by counting total epithelial cells by DAPI-stained nuclei, and cell sub-types among them were quantified by counting Sox9 + cells and PCNA+/Sox9- cells, in at least 10 villi from 3 replicates in each treatment group, at each timepoint. Post-Hatch, DAPI-stained nuclei, Sox9 + cells and PCNA+/Sox9- cells were quantified in at least 10 crypts and 10 villi from 3 replicates in each treatment group, at each timepoint. Cell sub-type percentages were calculated by dividing the number of each cell sub-type by the number of DAPI-stained villus/crypt cells.

In-situ Hybridization and Mucin Staining

Jejunum sections were deparaffinized by Histochoice® (Sigma-Aldrich, Rehovot, Israel) and rehydrated in a graded series of ethanol in DEPC-treated water (Sigma-Aldrich, Rehovot, Israel). RNAscope® in-situ hybridization (ISH) was performed as described by Wang et al. (35), according to the manufacturer's protocol (https://acdbio.com). Lgr5 mRNA transcripts were hybridized using a Gg-Lgr5 probe (XM_425441.4, Cat. No. 480781) and detected using RNAscope 2.5 HD Kit-RED (Cat. No. 322350). PepT1 mRNA transcripts were hybridized using a Gg-SLC15A1 probe (NM_204365.1, Cat. No. 462341) and detected using RNAscope 2.5 HD Kit-BROWN (Cat. No. 322300). A positive control probe (Gg-PPIB, Cat. No 453371) and a negative control probe DapB (Cat. No. 310043) were used for validation. Tissues were counterstained with 50% hematoxylin (Sigma-Aldrich, Rehovot, Israel) and sealed with DPX mounting medium (Sigma-Aldrich, Rehovot, Israel). For goblet cell quantification, tissues were stained with alcian blue (AB; A5268, Sigma-Aldrich, Rehovot, Israel) for 15m, rinsed in PBS and sealed with DPX mounting medium (Sigma-Aldrich, Rehovot, Israel).

Analysis of Cell Marker Localizations and Densities

Images were acquired by BX40 Olympus microscope (Waltham, MA, USA) at X100 and X400 magnification with a DP73 camera and processed with cellSense Imaging Software (version 1.16). For examining the distribution of Lgr5 expression in the embryonic villi at E19, total villi lengths were measured and divided into equal thirds for determining the bottom, middle and top villi regions. The percentage of Lgr5 punctate expression in each region was calculated by dividing punctate Lgr5 expression counts in each region by total villus punctate Lgr5 expression counts. For examining the extent of PepT1 expression in the embryonic villi at E19, lengths of the PepT1 + region and the PepT1- region were measured. The percentage of the PepT1 + region within the villus was calculated by dividing the PepT1 + region length by total villus length. For quantifying goblet cells, AB-stained mucins were counted in each villus. Goblet cell densities were calculated by dividing the number of villus goblet cells by villus length.

Statistical Analyses

Data were analyzed using one-way analysis of variance (ANOVA). Differences were considered significant at $P < 0.05$. Post-hoc Tukey-Kramer HSD tests were conducted for detecting significant differences between treatment groups at each timepoint. Significant differences were marked with different uppercase letters. Graphical data were expressed as mean ± standard error means (SEM). All statistical analyses were conducted with JMP Pro 15 software (SAS Institute, Cary, NC, USA).

Results

The pre-Hatch SI epithelium was visualized at E17 and E19 by combined immunofluorescence of proliferation marker PCNA and multipotent (MP) cell marker Sox9, along with DAPI nuclear staining. The majority of epithelial cells were PCNA+, and cells at the lower portion of the villus which co-expressed PCNA and Sox9 were regarded as MP cells (Fig. 2A,B, arrowheads). PCNA+/Sox9- cells at the upper region of the villus were regarded as progenitor cells (Fig. 2A,B, arrowhead outlines).

Examinations of effects of IOF treatments on the pre-Hatch SI epithelium revealed that at E19, total villus cell counts increased significantly by 19% in IOF-NaCl embryos ($P = 0.0046$), 33% in IOF-Leu embryos ($P < 0.0001$) and 40% in IOF Gln embryos ($P < 0.0001$) in comparison to Control embryos (Fig. 2C). Among these cells, Sox9 + MP cells, were significantly more abundant as a result of IOF treatments: in comparison to Control embryos, MP cell counts increased by 38% in IOF-NaCl embryos, 50% in IOF-Leu embryos and 52% in IOF-Gln embryos ($P < 0.0001$) (Fig. 2C). Furthermore, the percentages of MP cells, relative to total villus cell counts, increased from 38–44% in all treatment groups (IOF-NaCl: $P = 0.0152$; IOF-Leu: $P = 0.0182$; IOF-Gln: $P = 0.0388$) (Table 1).

IOF-Gln embryos also exhibited a significant, 36% increase in PCNA+/Sox9- progenitor cell counts, compared to Control embryos ($P = 0.0007$), while the other IOF treatment groups did not differ from Control embryos (Fig. 2C). Their percentages, relative to total villus cell counts, were stable between all groups (22–27%) (Table 1).

Comparisons of Control embryos between E17 and E19 revealed that MP cell counts and progenitor cell counts significantly increased with age ($P < 0.0001$) (Fig. 2C), and the percentages of MP cells increased significantly from 29–38% ($P < 0.0001$) while progenitor cell counts remained stable (25–27%) (Table 1). These results indicate that by further increasing total cell counts and expanding the Sox9 + multipotent cell niche at E19, IOF treatments induced early maturation of the SI epithelium.

Post-hatch, the SI epithelium had formed distinct crypts, in which Sox9 + MP cells were located at the bottom region and PCNA+/Sox9- progenitor cells were scattered throughout the crypt epithelium (Fig. 3C,D). The post-hatch villi were devoid of MP cells, as all cells were Sox9-negative (results not shown), but contained proliferating (PCNA+) cells at their bottom regions (Fig. 3A,B).

Cell count analyses showed that IOF-Gln significantly increased total villus and crypt cell counts at post-hatch ages, in comparison to Control chicks: villi cell counts increased by 26% at DOH ($P = 0.029$), 28% at D1 ($P < 0.0001$) and 12% at D3 ($P = 0.0196$) (Fig. 3E), and crypt cell counts increased by 10% at DOH, D3 and D7 ($P = 0.0391$, $P = 0.0276$, $P = 0.0205$, respectively) (Fig. 3F). The sole effect of IOF-Leu and IOF-NaCl on post-hatch epithelial cell counts was a 16% increase in villi cells at D1, compared to Control chicks ($P = 0.0045$ and $P = 0.0196$, respectively) (Fig. 3E).

However, proliferating (PCNA+) villi cell counts and percentages in all IOF-treatment groups increased in comparison to Control chicks at varying post-hatch timepoints. IOF-NaCl chicks exhibited significant increases in proliferating villi cell counts at DOH, D1, D3 and D7 ($P = 0.0051$, $P < 0.0001$, $P = 0.016$, $P < 0.0001$, respectively) (Fig. 3E), with corresponding increases in their percentages, relative to total villi cells, at DOH, D1 and D7 ($P = 0.0348$, $P = 0.0041$, $P = 0.0019$, respectively) (Table 2). In IOF-Leu chicks, proliferating villus cell counts and percentages increased at D1 and D7 (counts: $P < 0.0001$; percentages: $P = 0.0002$, $P < 0.0001$, respectively) (Fig. 3E) (Table 2). In IOF-Gln chicks, proliferating villus cell counts were significantly higher at DOH, D1 and D3 ($P = 0.0148$, $P < 0.0001$, $P = 0.0078$, respectively) (Fig. 3E), while their percentages were significantly higher only at D1 ($P = 0.0123$) (Table 2). These results indicate that the effects of IOF treatments on total villi cell counts did not correspond with the proportions of proliferating villus cells.

Within crypt cells, MP (Sox9+) cell counts did not differ significantly between Control, IOF-Gln and IOF-Leu chicks (Fig. 3F). However, IOF-Leu chicks exhibited significant, 19% and 17% decreases in MP cell counts, compared to Control chicks, at DOH and D1, respectively ($P = 0.0242$, $P = 0.0059$, respectively) (Fig. 3F). MP cell percentages, relative to total crypt cells, were significantly lower in comparison to Control chicks in IOF-Gln at DOH and D3 ($P = 0.0349$, $P = 0.0355$, respectively), and in IOF-Leu chicks at DOH and D1 ($P = 0.0028$, $P = 0.0004$, respectively) (Table 3), in accordance with the increases in total crypt cell counts. Lastly, progenitor (PCNA+/Sox9-) cell counts and percentages remained stable between treatments at all post-hatch timepoints (Table 3).

To summarize, within the first week post-hatch, IOF-Gln elicited significant expansions of the SI epithelium, as shown at DOH, D1 and D3 in the villi and DOH, D3 and D7 in crypts, while IOF-Leu and IOF-NaCl only increased villi cell counts at D1. The underlying proliferating villus cells and MP crypt cells

exhibited minor and inconsistent changes in quantities and percentages at these timepoints, while crypt progenitor cell counts and percentages remained stable. These findings indicate that IOF of glutamine expanded the epithelial cell lining of embryonic villi while increasing the proportions of the underlying multipotent cell niche and expanding the progenitor cell populations, resulting in expansions of both the villus and crypt epithelium during the first week post-hatch.

Another indicatory factor of pre-hatch SI maturation is the compartmentalization of ISC and differentiated cell niches during embryonic development. In order to determine whether IOF influenced ISC localizations within the embryonic SI epithelium, we visualized stem cell marker Lgr5 by RNAscope® *in-situ* hybridization (ISH). As the quantity of Lgr5 punctate expression did not differ between treatment groups, we calculated the percentage of Lgr5 punctate expression within the bottom, middle and top regions of the embryonic villus, relative to total villus expression, in each treatment group (Fig. 4). Control embryos at E17 and E19 exhibited a similar distribution of Lgr5 expression between regions, while IOF-treated embryos exhibited a significant shift in expression towards the bottom region of the villus, in which percentage of Lgr5 expression significantly increased from 45% in Control embryos, to 64% in IOF-NaCl embryos ($P = 0.0007$), 71% in IOF-Leu embryos ($P < 0.0001$) and 76% in IOF-Gln embryos ($P < 0.0001$). Accordingly, the percentage of Lgr5 expression decreased in the middle region from 33% in Control embryos to 25% in IOF-NaCl embryos ($P = 0.0219$), 24% in IOF-Leu embryos ($P = 0.0058$) and 21% in IOF-Gln embryos ($P = 0.0021$), and further decreased in the top region from 22% in Control embryos to 11% in IOF-NaCl embryos, 5% in IOF-Leu embryos and 3% in IOF-Gln embryos ($P < 0.0001$) (Fig. 4C).

These results indicate that all IOF treatments caused a shift in the localization of Lgr5 + stem cells to the bottom region of the villi at E19, thus promoting the zonation of stem cells into dedicated regions. Furthermore, stem cell zonation was most prominent following IOF of glutamine.

Next, RNAscope® ISH of absorptive cell marker PepT1 and Alcian Blue (AB) staining for goblet cell mucins were conducted in Control and IOF-treated embryos in order to determine the effects of IOF on the localization and proportions of differentiated compartment of the embryonic villus. Robust PepT1 expression was evident at the top region and absent from the lower region of the embryonic villus epithelium (Fig. 5A). At E19, IOF-Gln and IOF-Leu embryos exhibited significant, 1.9-fold and 1.3-fold increases (respectively) in the length of the PepT1-expressing region of the villus (PepT1+), compared to Control embryos ($P = 0.0007$, $P < 0.0001$, respectively), while the PepT1 + region in IOF-NaCl did not differ from that of Control embryos (Fig. 5C). However, the non-PepT1-expressing (PepT1-) region of the villus was significantly longer in IOF-Leu embryos, compared to Control embryos ($P < 0.0001$), but was unaffected in IOF-Gln embryos (Fig. 5C). Therefore, the percentage of the PepT1 + region length, relative to total villus length, decreased from 86% in the Control group, to 65% in the IOF-Leu group ($P < 0.0001$), but did not significantly differ between the IOF-Gln group (91%) and the Control group, as well as the Pre-IOF group at E17 (94%) (Table 4). This indicates that, compared to Control embryos, IOF-Gln increased the total amount of PepT1 expression within the embryonic SI epithelium while maintaining a high percentage of PepT1 expression within each villus, while the increases in villi lengths of IOF-Leu embryos decreased the percentages of the PepT1 expressing region.

Goblet cells, stained by Alcian Blue (AB) mucin staining (Fig. 5B), did not differ in quantity between treatment groups at E19 (data not shown). However, their density decreased in the villi of the IOF-Gln group, compared to the Control group (P = 0.0274), while goblet cell densities in the IOF-NaCl and IOF-Leu groups did not differ significantly from the Control group (Fig. 5D). These results indicate that the expansion of the embryonic villus epithelium by IOF of glutamine increased the absorptive cell population, as identified by cellular PepT1 expression, but not the secretive goblet cell population, as identified by AB staining.

As for the post-hatch SI epithelium, Lgr5 expression was restricted to the crypts, PepT1 expression was robust throughout the entire villus and goblet cells were intermittently scattered throughout the entire epithelium. IOF treatments did not affect localizations and distribution of these cell populations between DOH to D7. Therefore, the effects of IOF on stem (Lgr5+) and differentiated (PepT1 + and goblet) cell populations were evident only in the embryonic villus, 48h post nutrient administration.

Discussion

This study has shown that pre-hatch administration of glutamine and leucine by *in-ovo* feeding (IOF) during a critical timepoint in small intestinal (SI) development enhanced peri-hatch SI maturation by expanding and compartmentalizing multipotent, proliferating and differentiated epithelial cell populations.

Characterization of multipotency (MP) and proliferation the pre-hatch SI epithelium by PCNA and Sox9 immunofluorescence revealed that among epithelial PCNA + proliferating cells, Sox9 + cells were located at the bottom half of the villi and Sox9- cells were located at the upper half of the villi. This epithelial structuring was comparable to that of the adult crypt in mammals, in which the basal region is mainly comprised of multipotent (MP) stem cells, and in the upper region, proliferating cells lose their stemness and transiently amplify towards a definitive, differentiated state (2). We therefore characterized Sox9 + cells as MP cells and PCNA+/Sox9- cells as progenitor cells.

IOF of glutamine (IOF-Gln) significantly affected the dynamics of SI cellular maturation at E19, 48h post-administration, as the quantities of total epithelial cells and the underlying MP and progenitor cells increased, along with an increase in the percentage of MP cells, relative to total epithelial cells, compared to Control embryos. These results indicate that glutamine availability in the intestinal lumen, following amniotic ingestion by IOF-Gln embryos, resulted in increased proliferation of MP cells, in accordance with findings from previous studies that showed direct stimulation of crypt cell proliferation by glutamine, following its uptake by SI epithelial cells (22). In addition to the higher quantities and percentages of MP cells, which indicate an increased potential to generate functional differentiated cells, the increased quantities of progenitor cells in IOF-Gln embryos indicate that a higher number of cells advanced beyond the MP niche towards a mature, differentiated state.

In order to further comprehend the effects of IOF-Gln on the developing MP cell niche, we Investigated the effects of IOF of glutamine on the expression of stem cell marker Lgr5. Though previous studies of

glutamine supplementation resulted in inconsistent or non-prominent effects on expression levels of Lgr5 (36), we were able to identity significant changes in the localizations of Lgr5 mRNA expression through RNAscope® ISH, a method that has been previously proven useful for high specificity ISC identification in chicken (37). We found that IOF-Gln significantly shifted Lgr5 expression towards the bottom region of the villus at E19, compared to Control embryos. An elegant study by Shyer et al. (2015) demonstrated that stem cell localizations shift towards the villus bottom during the final stages of chick embryonic development, as a result of morphometric expansions of the villi (38). Our results showed a similar pattern in the SI epithelium of IOF-Gln embryos at E19, in which Lgr5 expression was highly concentrated at the bottom regions and almost absent from villi tips, in comparison to the more uniform distribution of Lgr5 expression along the shorter villi of Control embryos. We hypothesize that the induced expansion of the villus epithelium in IOF-Gln embryos, compared to Control embryos, promoted stem cell zonation at villi bottoms through enhanced BMP signaling along the upper regions of the villi, which locally inhibit stem cell self-renewal by suppressing Wnt signaling (4, 38).

Visualization of differentiated cells by PepT1, a marker for absorptive intestinal cells (33), revealed robust expression at the top region of the embryonic villus epithelium, and expression ceased at the lower regions. This finding was in accordance with previous findings in chick embryos (39) and comparable to PepT1 expression in SI villi tips in mice (40). In IOF-Gln chicks, the PepT1 expressing region of the villus was significantly longer than in Control chicks, indicating increased differentiation into mature, absorptive cells.

This result may be explained by induction of BMP signaling through villus elongation, which promoted differentiation over stem cell self-renewal along the villus (4, 38). Furthermore, BMP suppression of stem cell self-renewal involves suppression of Akt activity (4). Similarly, glutamine supplementation was also found to decrease the levels of activated Akt (41, 42). Therefore, it is possible that IOF of glutamine enhanced the differentiation of villi cells by inhibiting stem cell self-renewal along the villus through BMP and Akt-mediated signaling.

In contrast, IOF-Gln did not alter the number of goblet cells in the embryonic villus. Since the villi of IOF-Gln embryos were composed of a significantly higher number of cells, goblet cell densities in IOF-Gln embryos were significantly lower than in Control embryos. Similar to our findings, glutamine supplementation in weaning mice did not affect goblet cell counts (43), and goblet cell formation in murine enteroids was independent of glutamine (44). We therefore conclude that IOF-Gln specifically promoted differentiation of the absorptive cell lineage over the secretory cell lineage, possibly through Notch-mediated signaling (45).

IOF of leucine (IOF-Leu) also resulted in enhanced SI maturation at E19 through increased cellular proliferation and differentiation, compared to Control embryos, but to a lesser extent than IOF of glutamine. IOF-Leu increased total epithelial cell counts and Sox9 + MP cell counts and percentages, relative to total cell counts, in comparison to Control embryos. However, villus cell quantities were lower than in IOF-Gln embryos. Moreover, PCNA+/Sox9- progenitor cell quantities in IOF-Leu embryos did not

differ from Control embryos, in contrast to IOF-Gln embryos. This result indicates that despite the increased proportions of MP cell niche, the quantities of cells that transitioned from multipotency towards differentiation did not differ from those in Control embryos, indicating a limited effect of IOF-Leu on SI epithelial maturation at E19.

A possible explanation for the differences between the effects of IOF-Leu and IOF-Gln can be derived from the fact that dietary leucine acts as a nitrogen donor for glutamine synthesis (46). Therefore, IOF-Leu may have promoted the molecular pathway of glutamine-induced cellular proliferation in the SI epithelium in an indirect manner, resulting in decreased efficiency, compared to IOF-Gln.

Another possible explanation is that the maximal effect of leucine supplementation on SI proliferation may require an addition of other branched-chain amino acids (BCAAs), isoleucine and valine. We base this hypothesis on previous findings in pigs, which showed that leucine supplementation was most effective in enhancing epithelial cell proliferation when combined with isoleucine and valine (47). Furthermore, amino acid profiling of the amniotic fluid of E17 chick embryos revealed that leucine content was higher than isoleucine and valine (48). These data indicate that amniotic administration of an additional 6 mg of leucine by IOF may have disrupted BCAA ratios, resulting in a reduced induction of SI epithelial proliferation, compared to the potential effects of IOF of leucine combined with other BCAAs.

IOF-Leu did, however, promote stem cell zonation in a manner similar to IOF-Gln, as was visualized by Lgr5 expression. This result may also be attributed to the significant expansions in the villus epithelium in IOF-Leu chicks, compared to Control chicks, which may have shifted stem cell localizations towards the bottom of the villus through BMP signaling (38).

Examinations of differentiation at E19 by PepT1 expression, revealed that the proportions of the differentiated region of the villi were significantly smaller in IOF-Leu embryos, compared to IOF-Gln embryos. The PepT1 + region was shorter and the percentage of its length, relative to total villus length, was reduced, compared to IOF-Gln embryos. IOF-Leu therefore resulted in a slower rate of differentiation, compared to IOF-Gln embryos, and a reduced absorptive potential within their SI at E19. Additionally, goblet cell densities in IOF-Leu embryos did not differ from Control embryos, indicating that IOF of leucine did not affect the rate of goblet cell differentiation.

It should be noted that IOF of NaCl, the diluent for glutamine and leucine in the IOF solutions, also enhanced SI development at E19, 48h post-administration, through increased total epithelial cell counts, MP cell counts and percentages, relative to total villus cell counts, and zonation of Lgr5 mRNA at villus bottoms. However, proliferating cell counts and the extent of differentiation in IOF-NaCl embryos did not differ from Control embryos. The beneficial effects of IOF-NaCl on SI epithelial maturation may be attributed to enhanced activity of nutrient transporters, mediated by increased levels of Na^+ and Cl^- ions in the intestinal lumen, following the ingestion of the NaCl-enriched amniotic fluid. A variety of nutrient transporters, including Na-K+-ATPase and transporters for peptides, amino acids, sugars, vitamins and

minerals, depend on Na^+ and Cl^- ion exchange (49). Therefore, we hypothesize that IOF of NaCl induced SI epithelial proliferation through enhanced absorption of amniotic fluid nutrients.

Taken together, IOF elicited significant effects on SI development at E19, 48h post administration, in a nutrient-specific manner. While IOF of glutamine, leucine and NaCl promoted epithelial expansion and increased proliferation and zonation of the MP cell niche, only IOF of glutamine promoted cellular proliferation to the extent that significantly increased the progenitor cell population and promoted differentiation into absorptive cells.

These advancements in SI development at the final stage of embryonic development in IOF-Gln embryos further impacted the SI epithelium during the first week post-hatch, in which total villus cell counts were significantly higher at DOH, D1 and D3, and total crypt cell counts were significantly higher at DOH, D3 and D7, compared to Control chicks. In contrast, IOF of leucine and NaCl only increased villi cell counts at D1. Increased villus cell counts at D1 were previously found to be a result of primary feeding (11), therefore the combination of IOF and primary exogenous feeding may have elicited a prominent effect within the first 24h post-hatch. Furthermore, general decreases in the percentages of crypt MP cells and villus proliferating cells were observed during the first week post-hatch, in accordance with previous studies (5, 11), and were inconsistently affected by IOF, indicating that the effects of IOF on cellular proliferation and differentiation is most prominent pre-hatch.

Nevertheless, since the post-Hatch SI epithelium in all groups portrayed similar stem, proliferating and differentiated cell localizations, which were in accordance with previous studies (6, 11, 36, 39, 50), the expanded post-Hatch SI epithelium in IOF-Gln chicks was made up of a larger PepT1-expressing surface area, indicating a greater absorptive capacity, compared to Control chicks.

Improved nutrient utilization during the critical period of transition from egg-based nutrition to exogenous feed can alleviate the nutritional and energetic limitations that broiler chicks face during this period (51). IOF is therefore a highly applicative method for supporting SI development during the critical peri-hatch period, in order to improve SI functionality and nutrient utilization during the transition from egg-based nutrition to exogenous feeding. Furthermore, IOF provides an important tool for examining a variety of effects of specific nutrients and metabolites on SI epithelial development, functionality, immunity and microbial interactions (52, 53). This study is the first to uncover a cellular basis for the stimulatory effects of IOF on SI maturation, thus shedding light on the link between primary nutritional stimulation and SI development.

List Of Abbreviations

DAB, ,3'-diaminobenzidine (DAPI, 4',6-diamidino-2-phenylindole; DOH, day of Hatch; Gln, glutamine; IOF, *in-ovo* feeding; ISCs, intestinal stem cells; Leu, leucine; Lgr5, leucine-rich repeat containing G-protein coupled receptor 5; MAPK, mitogen-activated protein kinase; MP, multipotent; mTOR, mechanistic Target of

Rapamycin; PCNA, proliferating cell nuclear antigen; PepT1, peptide transporter 1; SEM, standard error mean; SI, small intestine; Sox9, SRY-box transcription factor 9.

Declarations

Acknowledgements

The authors' contributions were as follows: N.R. designed and conducted research, collected and analyzed data and prepared manuscript; T.M.Z. collected and analyzed data and assisted in manuscript preparation; J.D. assisted in research conduction; E.A.W. provided reagents and training for RNAscope® methodologies and assisted in manuscript preparation; Z.U. had primary responsibility for final content.

Ethics approval

All treatment and handling of animals were conducted according to established guidelines for animal care and handling by the Hebrew University Institutional Animal Care and Use Committee (IACUC:AG-17-15355-2).

Consent for publication

Not applicable.

Availability of data and material

The datasets used and/or analyzed during the current study are available from the corresponding author on reasonable request.

Competing interests

The authors declare that they have no competing interests.

Funding

This research was supported by Research Grant No. US-5074-18CR from the United States-Israel Binational Agricultural Research and Development Fund (BARD).

Authors' contributions

The authors' contributions were as follows: N.R. designed and conducted research, collected and analyzed data and prepared manuscript; T.M.Z. collected and analyzed data and assisted in manuscript preparation; J.D. assisted in research conduction; E.A.W. provided reagents and training for RNAscope® methodologies and assisted in manuscript preparation; Z.U. had primary responsibility for final content.

Acknowledgements

Not applicable.

References

1. Potten CS, Loeffler M. Stem cells: attributes, cycles, spirals, pitfalls and uncertainties. Lessons for and from the crypt. Development. 1990;110(4):1001-20.
2. Carulli AJ, Samuelson LC, Schnell S. Unraveling intestinal stem cell behavior with models of crypt dynamics. Integr Biol (Camb). 2014;6(3):243-57. doi: 10.1039/c3ib40163d.
3. Haramis AP, Begthel H, van den Born M, van Es J, Jonkheer S, Offerhaus GJ, Clevers H. De novo crypt formation and juvenile polyposis on BMP inhibition in mouse intestine. Science. 2004;303(5664):1684-6. doi: 10.1126/science.1093587.
4. He XC, Zhang J, Tong WG, Tawfik O, Ross J, Scoville DH, Tian Q, Zeng X, He X, Wiedemann LM, Mishina Y, Li L. BMP signaling inhibits intestinal stem cell self-renewal through suppression of Wnt-beta-catenin signaling. Nat Genet. 2004;36(10):1117-21. doi: 10.1038/ng1430.
5. Uni Z, Geyra A, Ben-Hur H, Sklan D. Small intestinal development in the young chick: crypt formation and enterocyte proliferation and migration. Br Poult Sci. 2000;41(5):544-51. doi: 10.1080/00071660020009054.
6. Uni Z, Smirnov A, Sklan D. Pre- and posthatch development of goblet cells in the broiler small intestine: effect of delayed access to feed. Poult Sci. 2003a;82(2):320-7. doi: 10.1093/ps/82.2.320.
7. Shyer AE, Tallinen T, Nerurkar NL, Wei Z, Gil ES, Kaplan DL, Tabin CJ, Mahadevan L. Villification: how the gut gets its villi. Science. 2013;342(6155):212-8. doi: 10.1126/science.1238842.
8. Geyra A, Uni Z, Sklan D. Enterocyte dynamics and mucosal development in the posthatch chick. Poult Sci. 2001a;80(6):776-82. doi: 10.1093/ps/80.6.776.
9. Geyra A, Uni Z, Sklan D. The effect of fasting at different ages on growth and tissue dynamics in the small intestine of the young chick. Br J Nutr. 2001b;86(1):53-61. doi: 10.1079/bjn2001368.
10. Uni Z, Tako E, Gal-Garber O, Sklan D. Morphological, molecular, and functional changes in the chicken small intestine of the late-term embryo. Poult Sci. 2003b;82(11):1747-54. doi: 10.1093/ps/82.11.1747.
11. Reicher N, Melkman-Zehavi T, Dayan J and Uni Z. It's All About Timing: Early Feeding Promotes Intestinal Maturation by Shifting the Ratios of Specialized Epithelial Cells in Chicks. Front. Physiol. 2020;11:596457. doi: 10.3389/fphys.2020.596457

12. Uni Z, and Ferket PR. Enhancement of development of oviparous species by in ovo feeding. 2003. North Carolina State Univ, Raleigh, NC, Yissum Research Development Company of the Hebrew Univ of Jerusalem, Jerusalem, IL, assignees. US Pat. No. 6,592,878. Washington, DC: US Patent and Trademark Office.
13. Hamilton HL. Lillie's development of the chick. An Introduction to Embryology. 1952, Revised by Hamilton, HL. H. Holt and Co., New York, NY.
14. Romanoff, AL. The Avian Embryo: Structural and Functional Development. 1960. Macmillan Co., New York, NY.
15. Tako E, Ferket PR, Uni Z. Effects of in ovo feeding of carbohydrates and beta-hydroxy-beta-methylbutyrate on the development of chicken intestine. Poult Sci 2004;83(13):2023-8. doi:10.1093/ps/83.12.2023.
16. Foye OT, Ferket PR, Uni Z. The effects of in ovo feeding arginine, beta-hydroxy-beta-methyl-butyrate, and protein on jejunal digestive and absorptive activity in embryonic and neonatal turkey poults. Poult Sci. 2007;86(11):2343-9. doi: 10.3382/ps.2007-00110.
17. Cheled-Shoval SL, Amit-Romach E, Barbakov M, Uni Z. The effect of in ovo administration of mannan oligosaccharide on small intestine development during the pre- and posthatch periods in chickens. Poult Sci. 2011;90(10):2301-10. doi: 10.3382/ps.2011-01488.
18. Kadam MM, Barekatain MR, Bhanja SK, Iji PA. Prospects of in ovo feeding and nutrient supplementation for poultry: the science and commercial applications–a review. J Sci Food Agric. 2013;93(15):3654-61. doi: 10.1002/jsfa.6301.
19. Gao T, Zhao M, Zhang L, Li J, Yu L, Lv P, Gao F, Zhou G. Effect of in ovo feeding of l-arginine on the hatchability, growth performance, gastrointestinal hormones, and jejunal digestive and absorptive capacity of posthatch broilers. J Anim Sci. 2017;95(7):3079-3092. doi: 10.2527/jas.2016.0465.
20. Dai D, Wu SG, Zhang HJ, Qi GH, Wang J. Dynamic alterations in early intestinal development, microbiota and metabolome induced by in ovo feeding of L-arginine in a layer chick model. J Anim Sci Biotechnol. 2020;11:19. doi: 10.1186/s40104-020-0427-5.
21. Wang J, Lin J, Wang J, Wu S, Qi G, Zhang H, Song Z. Effects of in ovo feeding of N-acetyl-L-glutamate on early intestinal development and growth performance in broiler chickens. Poult Sci. 2020;99(7):3583-3593. doi: 10.1016/j.psj.2020.04.003.
22. Rhoads JM, Wu G. Glutamine, arginine, and leucine signaling in the intestine. Amino Acids. 2009;37(1):111-22. doi: 10.1007/s00726-008-0225-4.
23. Rhoads JM, Argenzio RA, Chen W, Rippe RA, Westwick JK, Cox AD, Berschneider HM, Brenner DA. L-glutamine stimulates intestinal cell proliferation and activates mitogen-activated protein kinases. Am J Physiol. 1997;272(5 Pt 1):G943-53. doi: 10.1152/ajpgi.1997.272.5.G943.
24. Yi D, Hou Y, Wang L, Ouyang W, Long M, Zhao D, Ding B, Liu Y, Wu G. L-Glutamine enhances enterocyte growth via activation of the mTOR signaling pathway independently of AMPK. Amino Acids. 2015;47(1):65-78. doi: 10.1007/s00726-014-1842-8.

25. Coëffier M, Claeyssens S, Bensifi M, Lecleire S, Boukhettala N, Maurer B, Donnadieu N, Lavoinne A, Cailleux AF, Déchelotte P. Influence of leucine on protein metabolism, phosphokinase expression, and cell proliferation in human duodenum. Am J Clin Nutr. 2011;93(6):1255-62. doi: 10.3945/ajcn.111.013649.
26. Domeneghini C, Di Giancamillo A, Bosi G, Arrighi S. Can nutraceuticals affect the structure of intestinal mucosa? Qualitative and quantitative microanatomy in L-glutamine diet-supplemented weaning piglets. Vet Res Commun. 2006;30(3):331-42. doi: 10.1007/s11259-006-3236-1.
27. Sun Y, Wu Z, Li W, Zhang C, Sun K, Ji Y, Wang B, Jiao N, He B, Wang W, Dai Z, Wu G. Dietary L-leucine supplementation enhances intestinal development in suckling piglets. Amino Acids. 2015;47(8):1517-25. doi: 10.1007/s00726-015-1985-2.
28. Bartell SM, Batal AB. The effect of supplemental glutamine on growth performance, development of the gastrointestinal tract, and humoral immune response of broilers. Poult Sci. 2007;86(9):1940-7. doi: 10.1093/ps/86.9.1940.
29. Chang Y, Cai H, Liu G, Chang W, Zheng A, Zhang S, Liao R, Liu W, Li Y, Tian J. Effects of dietary leucine supplementation on the gene expression of mammalian target of rapamycin signaling pathway and intestinal development of broilers. Anim Nutr. 2015;1(4):313-319. doi: 10.1016/j.aninu.2015.11.005.
30. Kubben FJ, Peeters-Haesevoets A, Engels LG, Baeten CG, Schutte B, Arends JW, Stockbrügger RW, Blijham GH. Proliferating cell nuclear antigen (PCNA): a new marker to study human colonic cell proliferation. Gut. Apr;35(4):530-5. doi: 10.1136/gut.35.4.530.
31. Blache P, van de Wetering M, Duluc I, Domon C, Berta P, Freund JN, Clevers H, Jay P. SOX9 is an intestine crypt transcription factor, is regulated by the Wnt pathway, and represses the CDX2 and MUC2 genes. J Cell Biol. 2004;166(1):37-47. doi: 10.1083/jcb.200311021.
32. Barker N, van Es JH, Kuipers J, Kujala P, van den Born M, Cozijnsen M, Haegebarth A, Korving J, Begthel H, Peters PJ, Clevers H. Identification of stem cells in small intestine and colon by marker gene Lgr5. Nature. 2007;449(7165):1003-7. doi: 10.1038/nature06196.
33. Fei, YK, Sugawara M, Liu JC, Li HW, Ganapathy V, Ganapathy ME, Leibach FE. cDNA structure, genomic organization, and promoter analysis of the mouse intestinal peptide transporter PEPT1. Biochim. Biophys. Acta. 2000;1492:145–54. doi: 10.1016/s0167-4781(00)00101-9
34. Yair R, Shahar R, Uni Z. In ovo feeding with minerals and vitamin D3 improves bone properties in hatchlings and mature broilers. Poult Sci. 2015;94(11):2695-707. doi: 10.3382/ps/pev252.
35. Wang F, Flanagan J, Su N, Wang LC, Bui S, Nielson A, Wu X, Vo HT, Ma XJ, Luo Y. RNAscope: a novel in situ RNA analysis platform for formalin-fixed, paraffin-embedded tissues. J Mol Diagn. 2012;14(1):22-9. doi:10.1016/j.jmoldx.2011.08.002.
36. Chen Y, Tsai YH, Tseng BJ, Tseng SH. Influence of Growth Hormone and Glutamine on Intestinal Stem Cells: A Narrative Review. Nutrients. 2019;11(8):1941. doi: 10.3390/nu11081941.
37. Zhang H, Wong EA. Identification of cells expressing OLFM4 and LGR5 mRNA by in situ hybridization in the yolk sac and small intestine of embryonic and early post-hatch chicks. Poult Sci.

2018;97(2):628-633. doi: 10.3382/ps/pex328.

38. Shyer AE, Huycke TR, Lee C, Mahadevan L, Tabin CJ. Bending gradients: how the intestinal stem cell gets its home. Cell. 2015;161(3):569-580. doi: 10.1016/j.cell.2015.03.041.
39. Zhang, H, Wong, EA. Spatial transcriptional profile of PepT1 mRNA in the yolk sac and small intestine in broiler chickens. Poult. Sci. 2017;96,2871–2876. doi: 10.3382/ps/pex056.
40. Moor AE, Harnik Y, Ben-Moshe S, Massasa EE, Rozenberg M, Eilam R, Bahar Halpern K, Itzkovitz S. Spatial Reconstruction of Single Enterocytes Uncovers Broad Zonation along the Intestinal Villus Axis. Cell. 2018;175(4):1156-1167.e15. doi: 10.1016/j.cell.2018.08.063.
41. Larson SD, Li J, Chung DH, Evers BM. Molecular mechanisms contributing to glutamine-mediated intestinal cell survival. Am J Physiol Gastrointest Liver Physiol. 2007 Dec;293(6):G1262-71. doi: 10.1152/ajpgi.00254.2007. Epub 2007 Oct 4. PMID: 17916648; PMCID: PMC2432018.
42. Ren W, Yin J, Wu M, Liu G, Yang G, Xion Y, Su D, Wu L, Li T, Chen S, Duan J, Yin Y, Wu G. Serum amino acids profile and the beneficial effects of L-arginine or L-glutamine supplementation in dextran sulfate sodium colitis. PLoS One. 2014;9(2):e88335. doi: 10.1371/journal.pone.0088335.
43. Chen S, Xia Y, Zhu G, Yan J, Tan C, Deng B, Deng J, Yin Y, Ren W. Glutamine supplementation improves intestinal cell proliferation and stem cell differentiation in weanling mice. Food Nutr Res. 2018;62. doi: 10.29219/fnr.v62.1439.
44. Moore SR, Guedes MM, Costa TB, Vallance J, Maier EA, Betz KJ, Aihara E, Mahe MM, Lima AA, Oriá RB, Shroyer NF. Glutamine and alanyl-glutamine promote crypt expansion and mTOR signaling in murine enteroids. Am J Physiol Gastrointest Liver Physiol. 2015;308(10):G831-9. doi: 10.1152/ajpgi.00422.2014.
45. Stanger BZ, Datar R, Murtaugh LC, Melton DA. Direct regulation of intestinal fate by Notch. Proc Natl Acad Sci U S A. 2005;102(35):12443-8. doi: 10.1073/pnas.0505690102.
46. Nie C, He T, Zhang W, Zhang G, Ma X. Branched Chain Amino Acids: Beyond Nutrition Metabolism. Int J Mol Sci. 2018 Mar 23;19(4):954. doi: 10.3390/ijms19040954. PMID: 29570613; PMCID: PMC5979320.
47. Duan Y, Tan B, Li J, Liao P, Huang B, Li F, Xiao H, Liu Y, Yin Y. Optimal branched-chain amino acid ratio improves cell proliferation and protein metabolism of porcine enterocytesin vivo and in vitro. Nutrition. 2018;54:173-181. doi: 10.1016/j.nut.2018.03.057.
48. Omede AA, Bhuiyan MM, Lslam AF, Iji PA. Physico-chemical properties of late-incubation egg amniotic fluid and a potential in ovo feed supplement. Asian-Australas J Anim Sci. 2017;30(8):1124-1134. doi: 10.5713/ajas.16.0677.
49. Kiela PR, Ghishan FK. Physiology of Intestinal Absorption and Secretion. Best Pract Res Clin Gastroenterol. 2016;30(2):145-59. doi: 10.1016/j.bpg.2016.02.007.
50. Uni Z, Platin R, Sklan D. Cell proliferation in chicken intestinal epithelium occurs both in the crypt and along the villus. J Comp Physiol B. 1998;168(4):241-7. doi: 10.1007/s003600050142.
51. Moran ET Jr. Nutrition of the developing embryo and hatchling. Poult Sci. 2007;86(5):1043-9. doi: 10.1093/ps/86.5.1043.

52. Roto SM, Kwon YM, Ricke SC. Applications of In Ovo Technique for the Optimal Development of the Gastrointestinal Tract and the Potential Influence on the Establishment of Its Microbiome in Poultry. Front Vet Sci. 2016 17;3:63. doi: 10.3389/fvets.2016.00063.
53. Hou T, Tako E. The In Ovo Feeding Administration (Gallus Gallus)-An Emerging In Vivo Approach to Assess Bioactive Compounds with Potential Nutritional Benefits. Nutrients. 2018;10(4):418. doi: 10.3390/nu10040418.

Tables

Table 1. Multipotent and progenitor cell percentages in the embryonic SI epithelium of Control and IOF-treated embryos.

Age	Treatment	Multipotent Cells (%)	Progenitor Cells (%)
E17	Pre-IOF	28.6 ± 1.8^{C}	27.4 ± 2.2
E19	Control (non injected)	37.7 ± 1.4^{B}	25.4 ± 1
	IOF-NaCl	44 ± 1.1^{A}	27 ± 1.6
	IOF-Leu	43.9 ± 1.3^{A}	21.6 ± 1.7
	IOF-Gln	43.5 ± 1.3^{A}	26.7 ± 1.8

Cell percentages were calculated in the following manner: $\frac{\text{Cell sub-type quantities}}{\text{Total cell quantities}} \times 100$.

Values are means + SEM. Different uppercase letters mark significant differences in each cell sub-type by embryonic age and treatment by Tukey-Kramer HSD, $P<0.05$. No significant differences were found between values in each treatment group in progenitor cell percentages.

Table 2. Post-hatch villus proliferating cell percentages in Control and IOF-treated chicks.

	Proliferating Cells (%)			
Age	Control (non injected)	IOF-NaCl	IOF-Leu	IOF-Gln
Hatch	55.9 ± 6.6^{B}	72.5 ± 2.4^{A}	62.9 ± 3.4^{AB}	65.4 ± 4.5^{AB}
D1	44.3 ± 3.6^{B}	62.4 ± 3.7^{A}	68.7 ± 4.4^{A}	61.3 ± 3.9^{A}
D3	39.4 ± 2.9^{A}	47.9 ± 3.8^{A}	43.4 ± 1.5^{A}	46.5 ± 2^{A}
D7	15.7 ± 1.3^{C}	22.3 ± 1.5^{B}	29.6 ± 1.7^{A}	11.5 ± 0.6^{C}

Cell percentages were calculated in the following manner: $\frac{\text{Proliferating cell quantities}}{\text{Total villus cell quantities}} \times 100.$

Values are means + SEM. Different uppercase letters mark significant differences between treatment groups at each day by Tukey-Kramer HSD, $P<0.05$. No significant differences were found between values in each treatment group at each day in Proliferating Cell percentages.

Table 3. Multipotent and progenitor cell percentages in the crypt epithelium of Control and IOF-treated chicks.

	Multipotent Cells (%)				Progenitor Cells (%)			
Age	Control (non injected)	IOF-NaCl	IOF-Leu	IOF-Gln	Control (non injected)	IOF-NaCl	IOF-Leu	IOF-Gln
Hatch	67.5 ± 2.1^{A}	69 ± 1.8^{A}	56 ± 2.4^{B}	58.3 ± 2.7^{B}	19.6±1.6	14.6±1.4	19.6±1.7	16.4±1.6
D1	65.8 ± 1.8^{A}	66.8 ± 1.8^{A}	55.9 ± 1.8^{B}	60.3 ± 1.6^{AB}	19.7±1.8	20.9±1.6	25.6±1.9	19.7±1.4
D3	49.5 ± 2.5^{A}	48.5 ± 1.9^{A}	52.5 ± 1.9^{AB}	41.9 ± 1.5^{B}	31.6±.1.8	26.2±1.8	26.9±1.5	26.6±1.5
D7	28 ± 1.5^{AB}	31 ± 1.5^{A}	31.8 ± 1.5^{A}	23.8 ± 1.4^{B}	27.4±1.7	29.8±2.3	33.5±1.9	31.2±1.3

Cell percentages were calculated in the following manner: $\frac{\text{cell sub-type quantities}}{\text{Total crypt cell quantities}} \times 100.$

Values are means + SEM. Different uppercase letters mark significant differences between treatment groups at each day by Tukey-Kramer HSD, $P<0.05$. No significant differences were found between means in each treatment group at each day in Proliferating Cell percentages.

Table 4. Percentages of PepT1-expressing region lengths, relative to total villi lengths

Age	Treatment	PepT1+ Region (%)
E17	Pre-IOF	94.4±1.7^{A}
E19	Control (non injected)	85.8±2.4^{A}
	IOF-NaCl	72.5±1.9^{B}
	IOF-Leu	64.8±2.3^{B}
	IOF-Gln	90.6±1.5^{A}

Percentages of region lengths were calculated in the following manner:

$\frac{\text{PepT1+Segment Length (µm)}}{\text{Total villus length (µm)}} \times 100$. Values are means + SEM. Different uppercase letters mark significant differences by Tukey-Kramer HSD, $P<0.05$.

Figures

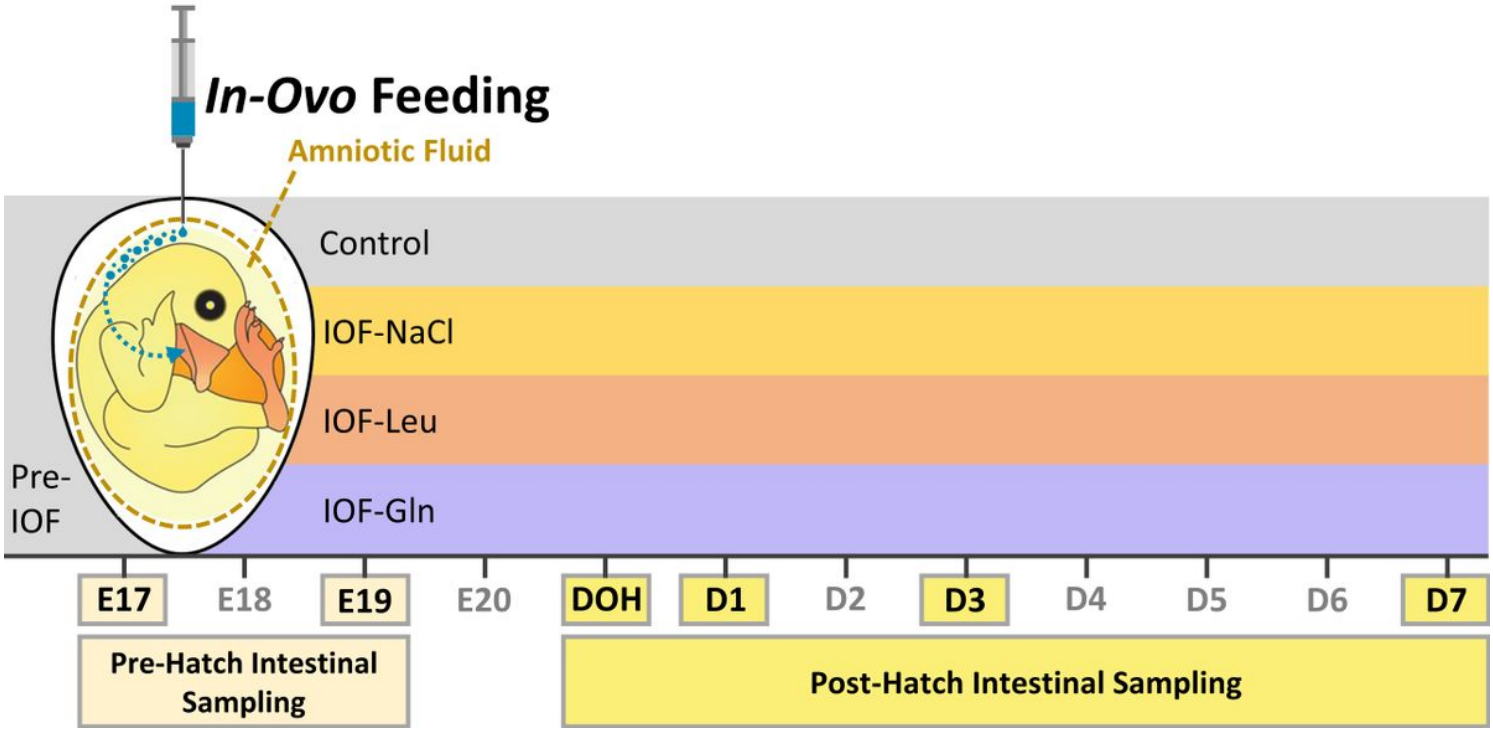

Figure 1

Description of experimental procedures. In-ovo feeding of glutamine (IOF-Gln, 1% glutamine in 0.4% NaCl), leucine (IOF-Leu, 1% leucine in 0.4% NaCl) and NaCl (IOF-NaCl, 0.75% NaCl) was conducted at embryonic day 17 (E17). Each nutrient solution was manually injected into the amniotic fluid. Intestinal sampling for downstream procedures was conducted at E17, prior to IOF treatments, and at E19, day of hatch (DOH), D1, D3 and D7 in Control (non-injected) and IOF treatment groups.

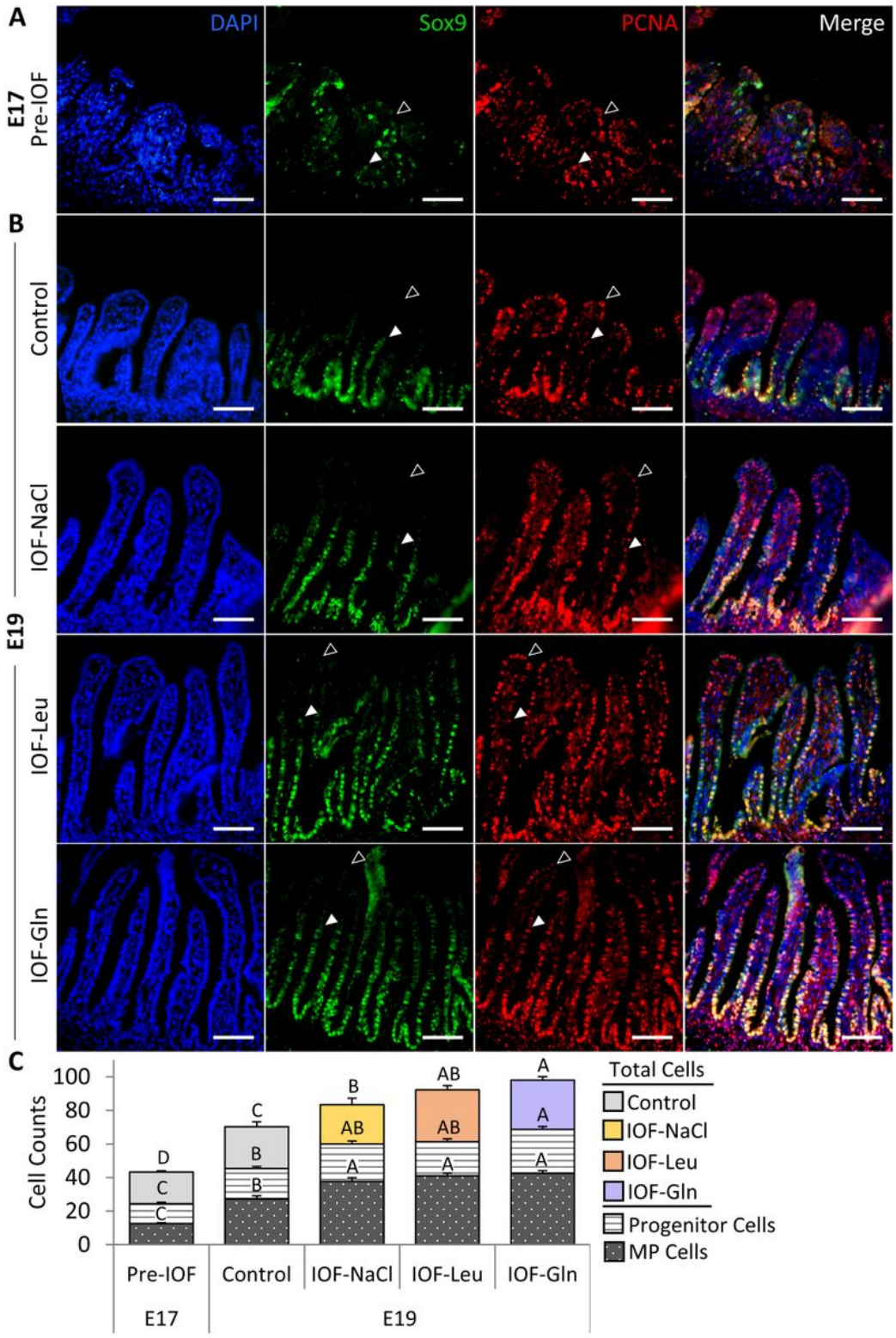

Figure 2

IOF increases pre-hatch SI epithelial cell quantities. Immunofluorescence of total jejunal epithelial cells by DAPI staining (blue), Sox9+ cells (green), PCNA+ cells (red), and Merged images at (A) E17 (pre-IOF) and at (B) E19 in Control (non-injected) IOF-NaCl =, IOF-Leu and IOF-Gln treated embryos. Multipotent (MP) Sox9+ cells were located from base to mid portion of each villus and co-localized with PCNA+ cells (arrowheads). Progenitor PCNA+/Sox9- cells were located from the mid to upper portion of each villus

(arrowhead outlines). Images were captured at X400 magnification. Scale bars, 50 μm. (C) Quantification of total epithelial cells, MP cells and progenitor cells at E17 (pre-IOF) and E19 (post-IOF). Values are means + SEM. Different uppercase letters mark significant differences between age/treatment group for each cell type by Tukey-Kramer HSD, P<0.05.

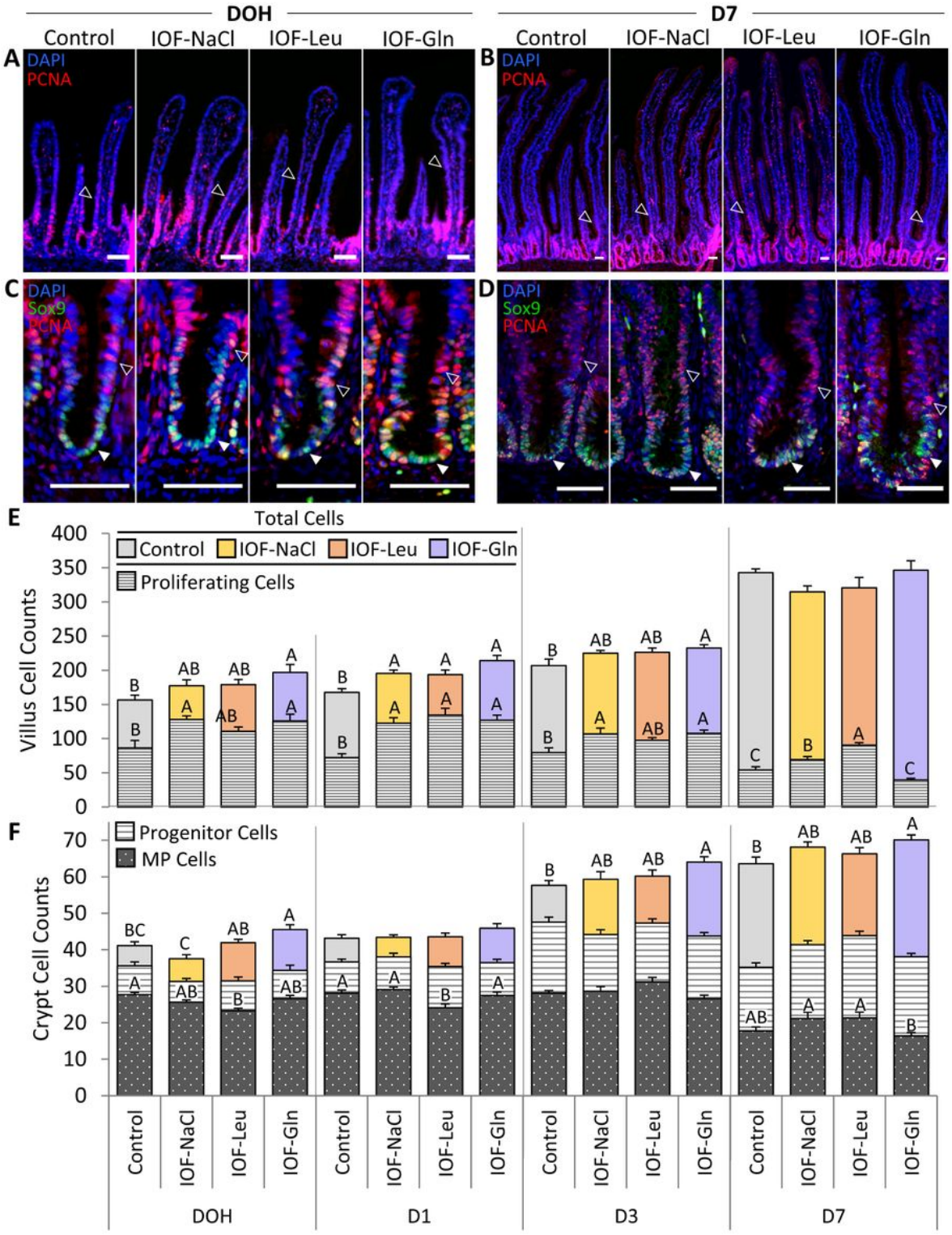

Figure 3

IOF increases post-hatch SI epithelial cell quantities. (A,B) Immunofluorescence of total villus epithelial cells by DAPI staining (blue), merged with PCNA+ staining (Red) at DOH (A) and D7 (B) in Control (non injected), IOF-NaCl, IOF-Leu and IOF-Gln treated chicks. Images were captured at X200 magnification and automatically stitched. Arrowhead outlines indicate PCNA+ proliferating cells at the bottom regions of the villi. (C,D) Immunofluorescence of total crypt epithelial cells by DAPI staining (blue), merged with PCNA+ staining (Red) and Sox9+ staining at DOH (C) and D7 (D) in Control, IOF-NaCl, IOF-Leu and IOF-Gln treated chicks. Images were captured at X400 magnification. Multipotent (MP) Sox9+ cells were located at the base of each crypt and co-localized with PCNA+ cells (C,D, arrowheads). PCNA+/Sox9- progenitor cells were scattered throughout the crypt epithelium (C,D, arrowhead outlines). Scale bars, 50 μm. (E) Quantification of total villus cells and villus proliferating cells from DOH to D7 in Control (non-injected) and IOF-treated chicks. (F) Quantification of total crypt cells, Sox9+ MP cells and PCNA+/Sox9- progenitor cells from DOH to D7 in Control (non-injected) and IOF-treated chicks. Values are means + SEM. Different uppercase letters mark significant differences between age/treatment group for each cell type by Tukey-Kramer HSD, P<0.05.

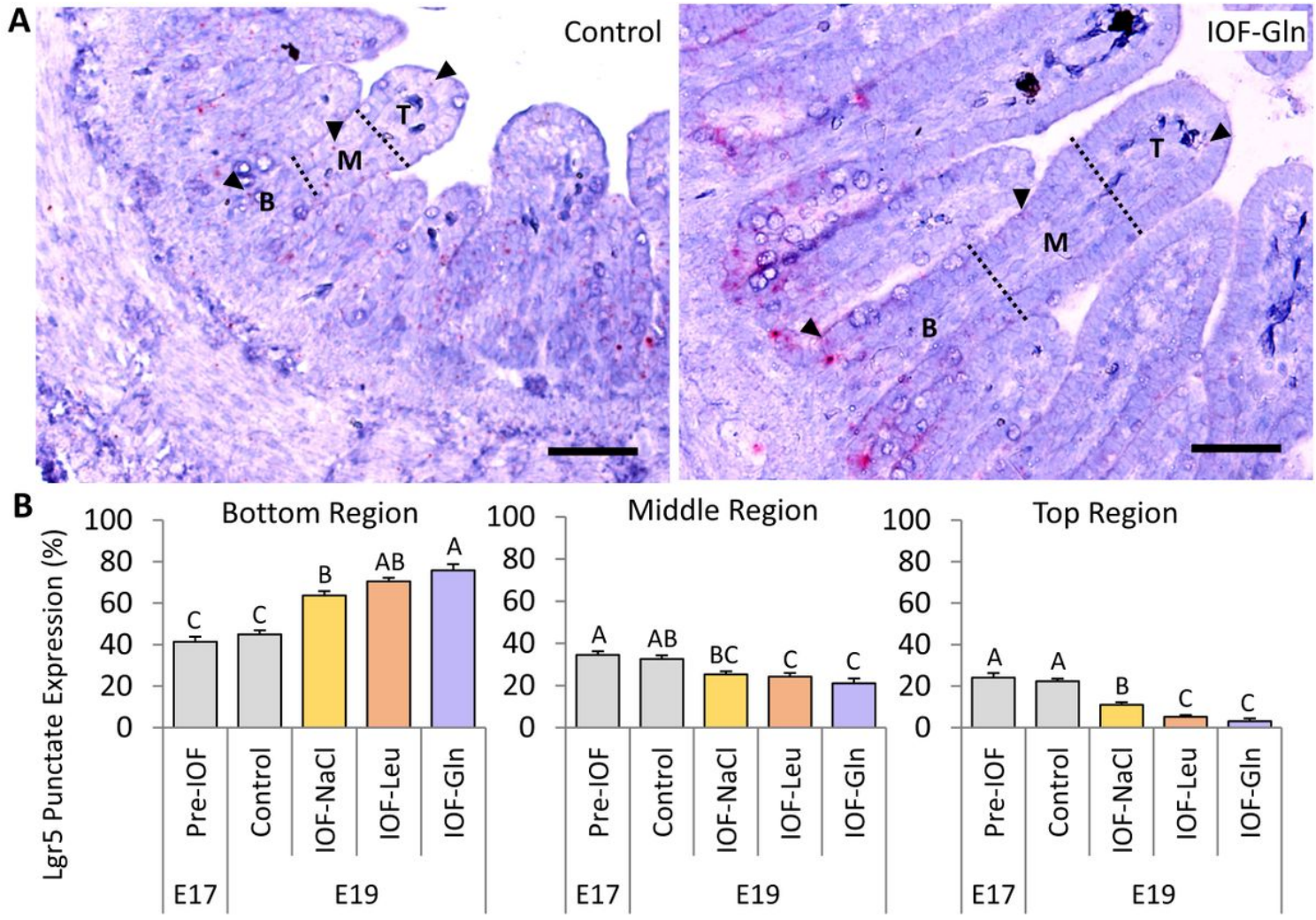

Figure 4

IOF shifts pre-hatch stem cell localizations toward villus bottoms. (A, B) Representative images of RNAscope® in-situ hybridization (ISH) of stem cell marker Lgr5 at E19 in the bottom (B), middle (M) and top (T) regions of each villus (separated by dotted lines) in Control (non-injected) (A) and IOF-Gln embryos (B). Arrowheads indicate Lgr5 punctate expression within each region. Lgr5 probes were visualized with fast-red and tissues were counterstained with hematoxylin. Images were captured at X200 magnification. Scale bars, 50 μm. (C) Percentage of Lgr5 punctate expression in each villus region, relative to total Lgr5 expression in the entire villus. Values are means + SEM. Different uppercase letters mark significant differences between age/treatment group in each villus region by Tukey-Kramer HSD, $P<0.05$.

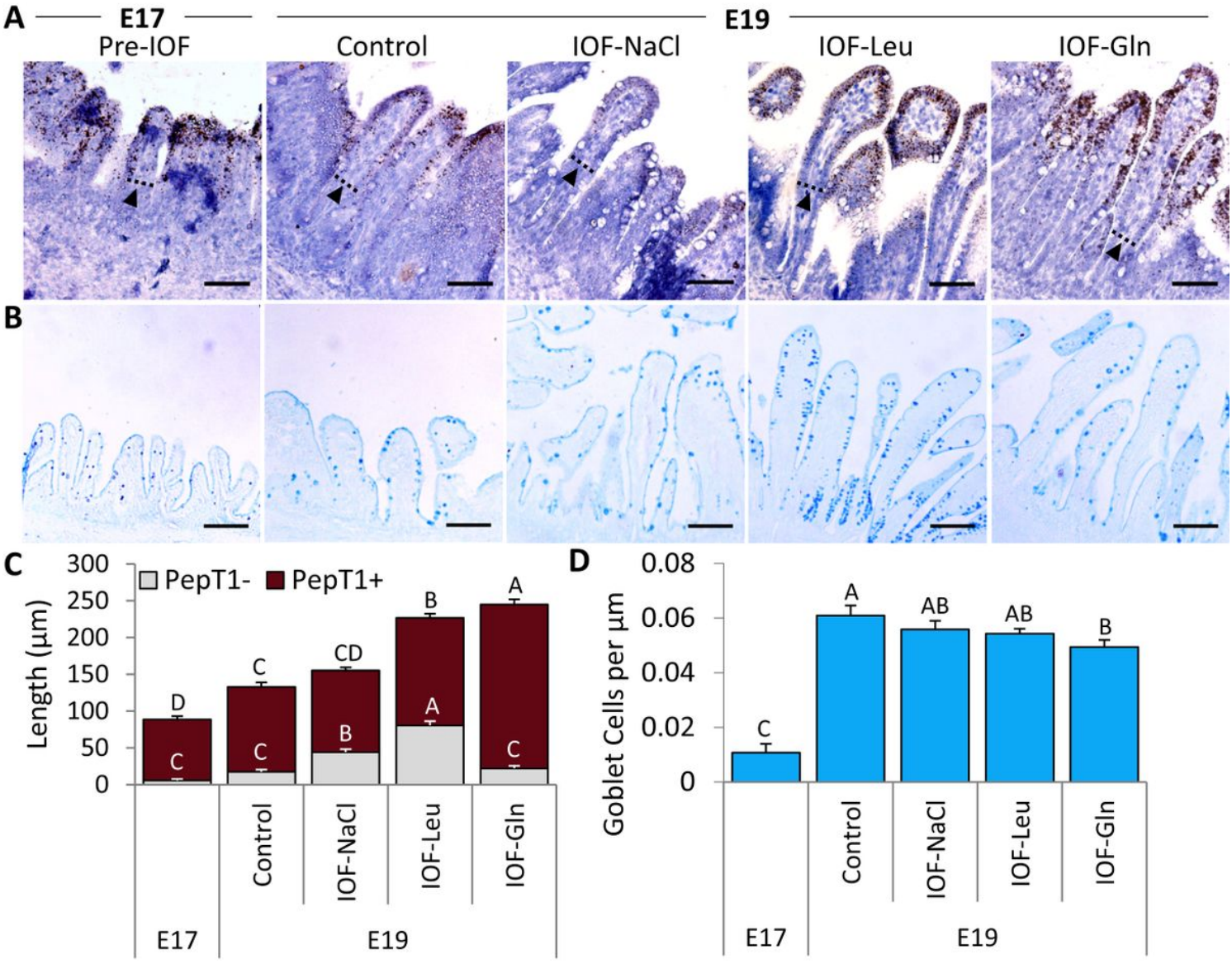

Figure 5

IOF lengthens pre-hatch absorptive cell marker expressing regions. (A) RNAscope® in-situ hybridization (ISH) of absorptive cell marker PepT1 at E17 (pre-IOF) and E19 in Control (non-injected), IOF-NaCl, IOF-Leu and IOF-Gln treated embryos. PepT1 probes were visualized with 3,3'-diaminobenzidine (DAB) and tissues were counterstained with hematoxylin. Dotted lines and arrowheads mark the limit between the

PepT1 expressing-region and non PepT1 expressing-region within the villus. (B) Goblet cells were visualized by Alcian Blue (AB) acidic mucin staining at E17 (pre-IOF) and E19 in Control (non-injected), IOF-NaCl, IOF-Leu and IOF-Gln treated embryos. Images were captured at X400 magnification. Scale bars, 50 μm. (C) Length of non-PepT1 expressing (PepT1-, grey) and PepT1-expressing (PepT1+, brown) segments within each villus at E17 (pre-IOF) and E19 in Control (non-injected) and IOF-treated embryos. (D) Goblet cell densities at E17 (pre-IOF) and E19 in Control (non-injected) and IOF-treated embryos. Values are means + SEM. Different uppercase letters mark significant differences between age/treatment group by Tukey-Kramer HSD, $P<0.05$.